The Fourth Australasian Ground Control in Mining Conference 2018

Paper Number: 94

The practicalities of effective stress measurement in rock

I Gray MAusIMM.

Managing Director, Sigra Pty Ltd, Acacia Ridge, Brisbane, Queensland 4110, ian@sigra.com.au

ABSTRACT

This paper examines the practical limitations that affect the measurement of stress in rock. As most rock stress measurement is conducted through the invasive process of drilling a hole in a rock mass, the nature of the rock and its response to being drilled form the basis of the stress measurement process. The prime techniques to measure stress down a borehole are to conduct hydraulic fracturing and its variant hydro-jacking, overcoring, and the examination of the borehole wall for breakout or tensile fracture. It is also possible in some circumstances to use the sonic velocity within the rock mass as an indicator of the stress situation. Other structural indicators of stress such as joints, faulting and intrusions are useful but may not reflect the current stress situation within the rock mass. The variability of stress within the rock mass also needs to be considered as it is quite unusual to have a monotonic stress situation throughout any rock mass. The outdated concept of measuring the far field stress in a few measurement for use in a numerical model is quite dangerous. It is essential to make multiple measurements and to generate an understanding of its distribution in some form of model before stress can sensibly be incorporated into underground design.

INTRODUCTION

The basic processes of stress measurement in rock are hydrofracture, hydrojacking, overcoring and borehole breakout. All of these techniques rely to a great extent on the linear and isotropic elastic response of the rock. Unfortunately, rocks tend to have fabric at multiple levels, and their stress strain behaviour is frequently non-linear and anisotropic. This non-linearity may ultimately lead to rock failure at the borehole wall, which is point of measurement.

The fundamental equations used in all four stress measurement systems are those which describe the state of stress around a borehole in linearly elastic, isotropic material which contains a stress field perpendicular to the borehole. These equations were developed by Kirsch (1898). They have been extended to permit the determination of the three dimensional stress state from overcoring, which includes strain gauges to measure the total state of strain at the borehole wall rather than just a measurement of diameter change. Nevertheless the equations and their assumptions of elastic linearity remain the same.

In reality rock is frequently non-linear, anisotropic and may exhibit poroelastic behaviour. The latter describes its deformation under varying fluid pressures within the rock mass. These departures from ideal material behaviour need to be considered, if not actually used, in every stress measurement analysis.

THE BASIC EQUATIONS

Stress and strain

The fundamental equation that describes the deformation of a linear elastic solid is given in Equation 1 where C is the compliance matrix .

$$\{\varepsilon_{ij}\} = [C_{ijkl}]\{\sigma_{kl}\} \tag{1}$$

For a general elastic solid there are six stresses and six engineering strains which are linked by either a compliance (Equation 1) or stiffness matrix, each with 36 terms. Because of the symmetry of these matrices the number of terms may be reduced to 21. This full form of the compliance matrix is very useful as it can express all manner of real relationships between stress and strain. For example, dilation or compaction can be expressed in terms of any of the shear stresses. Other relations that it may mathematically express are less obvious for those familiar with the simple isotropic definition of stress and strain theory, which has only a single value of Young's modulus and Poisson's ratio from which shear or bulk moduli may be described.
An intermediate form of compliance matrix lying between the fully expanded form of Equation 1 and the isotropic case is that of an orthotropic solid. This is shown in Equation 2.

$$\begin{Bmatrix} \varepsilon_{11} \\ \varepsilon_{22} \\ \varepsilon_{33} \\ \gamma_{23} \\ \gamma_{31} \\ \gamma_{12} \end{Bmatrix} = \begin{bmatrix} \frac{1}{E_1} & -\frac{\nu_{21}}{E_2} & -\frac{\nu_{31}}{E_3} & 0 & 0 & 0 \\ -\frac{\nu_{12}}{E_1} & \frac{1}{E_2} & -\frac{\nu_{32}}{E_3} & 0 & 0 & 0 \\ -\frac{\nu_{13}}{E_1} & -\frac{\nu_{23}}{E_2} & \frac{1}{E_3} & 0 & 0 & 0 \\ 0 & 0 & 0 & \frac{1}{G_{23}} & 0 & 0 \\ 0 & 0 & 0 & 0 & \frac{1}{G_{31}} & 0 \\ 0 & 0 & 0 & 0 & 0 & \frac{1}{G_{12}} \end{bmatrix} \begin{Bmatrix} \sigma_{11} \\ \sigma_{22} \\ \sigma_{33} \\ \tau_{23} \\ \tau_{31} \\ \tau_{12} \end{Bmatrix} \tag{2}$$

In this E_i represents the Young's modulus in the i direction.
ν_{ij} represents Poisson's ratio of negative *j* direction strain divided by *i* direction strain under uniaxial loading in the *i* direction.
G_{ij} represents the shear modulus between the *i* and *j* planes.

The orthotropic solid conveniently ignores 12 off diagonal terms of the 21 in the full compliance matrix thus leaving 9 independent terms.

In a further simplification the orthotropic matrix may be reduced to an isotropic case, in which case all the values of Young's moduli are equal as are all the values of Poisson's ratio. In this isotropic case the shear modulus is expressed in Equation 3.

$$G = \frac{E}{2(1+v)} \tag{3}$$

It should be noted that the shear modulus terms of the orthotropic case, G_{ij}, are independent, and the approximation of Equation 4 for the orthotropic case proposed by Huber (1923) is not rigorous.

$$G_{ij} = \frac{\sqrt{E_i E_j}}{2(1+\sqrt{\nu_{ij}\nu_{ji}})} \tag{4}$$

Effective stress and poroelasticity

In addition to the strain behaviour of a rock or coal from external stress, we need also to consider what effect changing fluid pressure within it has on its deformation. This deformation may be associated with the concept of effective stress. This is often only understood in soil mechanics terms as the total stress minus fluid pressure. This is a gross oversimplification for the case of rock, where Equation 5 may be used to describe the effective stress within the rock mass.

$$\sigma'_{ij} = \sigma_{ij} - \delta_{ij}\alpha_i P \tag{5}$$

Where σ'_{ij} is the effective stress acting on a plane perpendicular to the vector *i* in direction *j*

σ_{ij}	is the total stress acting on a plane perpendicular to the vector *i* in direction *j*
δ_{ij}	is the Kroneker delta. If $i \neq j$ then $\delta_{ij} = 0$, while if $i = j$ then $\delta_{ij} = 1$
α_i	is the poroelastic coefficient affecting the plane perpendicular to the vector *i*
P	is the fluid pressure in pores and fractures

The Kronecker delta term is used because a static fluid cannot transmit shear.
The directional subscript used for the poroelastic coefficient is not usual practice. Normally a scalar quantity is used based on volumetric measurement, and is called Biot's coefficient.

If we consider that deformation within a porous rock mass is due to effective stress alone and if in addition we consider the case of an orthotropic rock mass loaded orthogonally to its principal directions of stiffness, thus removing the shear terms, we can describe the strain brought about by a change in effective stress by Equation 6.

$$\Delta\varepsilon_{ii} = \frac{1}{E_i}\Delta\sigma'_{ii} - \frac{v_{ji}}{E_j}\Delta\sigma'_{jj} - \frac{v_{ki}}{E_k}\Delta\sigma'_{kk} \tag{6}$$

We must not confuse the effective stress described in Equation 6 with a real stress within the rock structure in the porous mass. The effective stress described is one that merely leads to the same deformation as total stress in a situation where fluid pressure within the rock mass does not change.

If we substitute the definition of principal stress from Equation 5 into Equation 6 we can get Equation 7 (Gray, 2017) which describes the change in deformation in terms of a change in total stresses and fluid pressure.

$$\Delta\varepsilon_{ii} = \frac{1}{E_i}\Delta\sigma_{ii} - \frac{v_{ji}}{E_j}\Delta\sigma_{jj} - \frac{v_{ki}}{E_k}\Delta\sigma_{kk} - \Delta P(\frac{1}{E_i}\alpha_i - \frac{v_{ji}}{E_j}\alpha_j - \frac{v_{ki}}{E_k}\alpha_k) \tag{7}$$

Against this background of what are still linear elastic equations that have been reduced by a lot of assumptions to six independent elastic coefficients plus three poroelastic coefficients we need to remember that real rocks are frequently not linearly elastic. Therefore the only way to model their behaviour is by a piecewise linear approach that must form part of a numerical model.

Stress and deformation around a borehole

The equations that form the basis of stress measurement around a borehole are based on an isotropic, linear elastic solid which has only two independent variables, Young's modulus, *E*, and Poisson's ratio, υ. The first of these equations describes the state of stress around a borehole wall in a biaxial stress field. Ignoring poroelastic effects this is given in Equation 8.

$$\sigma_T = \sigma_2\big(1 - 2Cos(2\theta)\big) + \sigma_3\big(1 + 2Cos(2\theta)\big) - P \tag{8}$$

Where	σ_T	is the tangential stress at the hole wall
	σ_2	is a principal stress acting perpendicularly to the borehole axis
	σ_3	is a principal stress acting perpendicularly to the borehole axis and perpendicularly to σ_2
	P	is the fluid pressure within the hole
	θ	is the angle measured from the direction of σ_2.

In a uniform field of σ_2 alone this reduces to equation (9).

$$\sigma_T = \sigma_2\big(1 - 2Cos(2\theta)\big) - P \tag{9}$$

When $\theta = 0^o\ or\ 180^o$ this has a value of $\sigma_T = -(\sigma_2 + P)$

When $\theta = \pm 90^o$ this has a value of $\sigma_T = 3\sigma_2 - P$

If $\sigma = \sigma_2 = \sigma_3$ then $\sigma_T = 2\sigma - P$ all around the borehole circumference.

In the event that $\sigma_3 < \sigma_2$ then if $\sigma_2 + P > 3\sigma_3$ a tensile stress is created at the hole wall at $\theta = 0^o$ or $\theta = 180^o$. If this tensile stress is above the tensile strength of the rock it may lead to tensile cracking.

More commonly the situation arises where the borehole wall is just in compression. If $\sigma_3 < \sigma_2$ then at $\theta = \pm 90^o$ the compressive stress at the hole wall becomes Equation 10.

$$\sigma_T = 3\sigma_2 - \sigma_3 - P \tag{10}$$

These equations form the basis of stress measurement by borehole breakout and hydrofracture.

Equation 11 describes the deformation around a borehole that has been stress relieved by overcoring (Jaeger and Cook, 1979).

$$\delta D = \frac{D}{E}[(\sigma_2 + \sigma_3) + 2(\sigma_2 - \sigma_3)(1 - \upsilon^2)\cos 2\theta - \upsilon\sigma_1] \tag{11}$$

Where δD	=	the change in diameter of the pilot hole
D	=	the borehole diameter
σ_2	=	the major stress perpendicular to the hole wall
σ_3	=	the minor stress perpendicular to the hole wall
σ_1	=	the stress in the direction of the axis of the hole
E	=	Young's modulus
υ	=	Poisson's ratio
θ	=	The angle from the axis in which σ_2 acts.

REAL ROCK PROPERTIES

Much of rock mechanics is founded upon the basis that rock is linearly elastic and isotropic up until brittle failure occurs. While this approximates the behaviour for some igneous and metamorphic rocks, the vast majority of sedimentary and metamorphic rocks have much more complex behaviour. Gray, Zhao and Liu (2018) have developed test methods to determine rock properties from core testing, based on the assumption that the rock behaves orthotropically. While this is a simplifying assumption it is far less so than an assumption that the rock is isotropic. The orthotropic assumption manages to capture the main components of anisotropy without the finer details of dilation etc. The testing presented in that paper showed that many sedimentary rocks are quite non-linearly elastic and some are poroelastic. Figure 1 from this paper shows the variation in axial modulus for a core of Sydney sandstone under differing axial and radial (confining) stress. This rock also shows poroelastic behaviour as shown in Figure 2. Some siltstones that have been tested show a stiffness along the bedding planes that is three times the axial stiffness.

While this work captures the nonlinear and anisotropic behaviour of the core specimen, it does not yet separate the effects of differing stresses that are perpendicular to the core axis.

ROCK STRESS MEASUREMENT

The four main methods of rock stress measurement are hydrofracture, hydrojacking, overcoring and borehole breakout. All these depend to some degree on Equations 8 to 10 which describe the stress around a hole. Overcoring depends on Equation 11 and extensions of it which describe strain around a hole.

Hydrofracture

Hydrofracture is a process by which a section of borehole is sealed and the fluid pressure in this section is raised until sufficient tensile stress is generated at the borehole wall that it overcomes the tensile strength of the rock and breaks. Fluid then generates a fracture that propagates away from the borehole wall. In a uniform isotropic rock the fracture will develop in a plane which has the minimum normal stress acting across it. As many rocks have pre-existing jointing or weaker planes which have a reduced tensile strength the fractures frequently follow these. Whether the fracture actually switches from one mode of development to another is dependent on the stresses and tensile strength of the rock in different directions and the stresses within it. The reality is that the fracture will go where it wants and that may be different orientation to that at the start of propagation.

The common, idealised behaviour of a hydrofracture test is shown in Figure 3. Here the hole is pumped at a constant rate until the pressure is sufficient that it overcomes the tensile strength of the borehole wall. The pressure then declines until pumping is stopped, when it drops off. The drop off is initially rapid and then it slows. The pressure drop off rate increase when the sides of the hydrofracture touch at the fracture closure pressure, and the system becomes much stiffer. This closure pressure is interpreted as equating to the minimum principal stress existing within the rock mass.

The closure pressure can in some cases be seen easily on a pressure versus time plot. More usually it requires some advanced analysis of the data to find. Determining the value of this pressure and stress has been the subject of much research and many papers. Currently the favoured approach in petroleum work is to use the G function (Nolte, 1979; Barree 1998; Barree et al 2009), or the square root approach (Hagoort 1981; Barree et al, 2009). These techniques have been developed generally to enable the minimum stress to be calculated from mini-fracs to assist hydrofracture design in the extraction of petroleum from low permeability reservoirs. The square root approach involves plotting functions of pressure and the first and second derivatives of pressure with respect to the square root of time versus the square root of time after shut in (the cessation of pumping and valve closure above the test zone).

The petroleum industry generally only conducts hydrofracturing through casing that has been cemented in place and subsequently perforated. There is no expectation that the fracture opening pressure will yield anything of use. The civil and mining industry tend to undertake hydrofracturing in boreholes that are unlined, using inflatable packers to seal the section of hole being tested. They expect that the fracture opening pressure is an important parameter that can be used in the determination of the major stress. The reasoning behind this is that if the minor stress can be determined from the fracture closure pressure then the major stress can be determined from Equation 10.

The general supposition made in examining fracture closure is that the rock will behave identically in multiple opening and closing cycles, with the exception that on the first cycle the tensile stress of the rock must be overcome.

This approach has many shortcomings:

- The first of these is that the stress distribution of Equation 10 actually applies. It is, after all, based upon linear elastic theory which may not apply to the rock being tested.
- The second shortcoming is that poroelastic effects can be ignored. In some rocks this is undoubtedly true. However, if poroelastic effects do exist, then leakage of fluid from the hole and the fracture into the rock alter the effective stress and may change its elastic properties.
- The third shortcoming is the presumption that the fracture opens and closes perfectly and the rock behaves identically on re-opening. Fragments of rock from the initial hydrofracture cycle will tend to drop into the fracture and prop it open. Also if the fracture propagates up a plane of natural weakness this plane is unlikely to be orientated perpendicular to the direction of minimum stress. As a consequence the shear stress on that failure plane will be removed on fracture opening and the plane will close with an offset. This means that the fracture does not close properly.
- The fourth is that the fracture re-opening pressure is dependent on the flow rate. From actual testing we generally see that the higher the flow rate, the higher the fracture re-opening pressure. We presume that at lower flow rates the fracture has time to pressurise and in doing so changes the stress distribution at the borehole wall, and as a consequence the entire mechanics of fracture re-opening.
- The fifth is the key assumption that the borehole axis lies on an axis of intersection between planes on which the minor and intermediate stresses act. If the minor stress is in any other orientation then the entire method of analysis fails.
- The sixth shortcoming is the effect which any flaw at the borehole wall has on fracture opening. Stress concentrations are real. While this does not affect the closure pressure, it may provide a point from which a fracture develops.

- Following from the fifth and sixth points, the reality is that while theoretically the pumped fluid pressure does not act to open up a fracture, it only takes a minor flaw in the rock for this to actually occur. This means that hydrofracture near surface tends to measure a minimum stress that is the overburden stress.

From a practical viewpoint the use of packers to seal a section of borehole requires the packers to be at a higher pressure than the injected fluid. This means that it is highly likely that the fracture will be initiated by the packer. Great care must be exercised in ensuring that the pressure that the packer applies to the hole wall is only slightly in excess of that of the contained fluid or this problem will ensue. This is an important hydrofracture design issue that is frequently ignored.

The real case where the fracture opening pressure is lower than the subsequent pressure that occurs while extending fractures is seldom considered. This occurs where the minimum tangential stress at the borehole wall is smaller than the minor stress in the rock mass. This occurs because of stress concentration effects around a hole and the distribution of stresses. Indeed it is possible to have a tensile stress before fracturing.

The problem of avoiding pre-existing planes of weakness in a hole may be considerable. Physical manufacturing limitations mean that straddle packer systems have to have some spacing between packers. This means that it is quite likely that one or several planes of weakness may be included within the straddled zone.

To determine the direction of the major stress from hydrofracture the hole needs to be examined by some means to determine the orientation of the fractures. This used to be accomplished using an impression packer but is more usually achieved using an acoustic scan of the hole. If the scan shows that the fracture that is formed is not in line with the hole axis then it means the simple analysis for major stress based on Equation 10 will not apply.

The process of using a constant flow rate during injection was developed to suit the lack of control that used to exist with pumping equipment. In a borehole with little leakage the preferred system is to ramp up the pressure until breakdown occurs and flow can be observed. This approach does not work if the test zone has fractures that leak off at a rate that is proportional to the pressure.

Hydrojacking

Hydrojacking involves using packers to straddle a section of borehole that contains a transecting fracture. The zone is then pressurised to open the fracture. After opening, pumping ceases and the closure pressure is determined to find the normal stress across the fracture. The hope is that several fractures of differerent orientations exist and can be individually tested so that adequate measurements are made to enable the derivation of the stress tensor.

In reality this can seldom be achieved because most rock has only one to three fracture groups. It also means that the prime advantage of the technique which is to obtain a value of stress in fractured rock, is lost. Hydrojacking is of particular use where there are pre-existing fractures that make hydrofracture impossible and would prevent the use of overcoring.

In testing fractured rock the process is more normally to run an acoustic scan of the borehole to determine what fractures are present and then to choose a zone to test which will in all probability contain a few fractures. This is then tested by hydrojacking and the acoustic scan is then run again to see what fractures have opened. Determining which fractures have opened can be difficult and may not be possible. The end result is frequently a closure pressure signal that is made up of several components probably caused by sequential or simultaneous closure on several fractures. Figure 4 shows the pre and post hydrojacking acoustic scans of such a complex fractured section. Determining which fractures opened is very difficult.

One practical limitation of hydrojacking zones of a borehole with conjugate fracture sets using a packer system is the risk of a wedge of rock being dislodged from the hole wall and jamming the packer system in the hole. This problem may be overcome by cementing plugs above and below the test zone and testing through tubing cemented through the top plug. If the fractures are too open this is impossible because the grout is lost into the rock.

Despite these limitations hydrojacking can be usefully used to gain some idea of stress in fractured rock.

Overcoring

Overcoring is an indirect means of measuring stress because it involves the measurement of deformation associated with stress relief. To convert the deformation into stress requires the determination of the rock properties.

Surface overcoring

This is a useful process that is generally forgotten. It involves gluing a strain gauge to the surface of a smoothed rock face. An initial strain reading is taken along with rock temperature measurement. A concrete core drill is then used to drill over the strain gauge and temperature sensor and strain measurement recommences with temperature monitoring. The core is then taken for the measurement of Young's modulus and Poisson's ratio. This is a simple test which yields the biaxial stress state at the surface of the opening. This is sometimes a more useful measurement than one made remotely as it provides the stress right at the wall of an excavation.

Pilot hole overcoring

This process involves testing at the end of a borehole. It involves drilling a pilot hole from the end of the hole. Some form of cell is inserted into the pilot hole to take initial pilot hole diameter or strain measurements. The pilot hole is then overcored at the original hole diameter thus relieving all stresses. The core deforms during this process and the deformation is measured using either strain gauges or by pins that bear on the pilot hole wall. The process is shown in more detail in Figure 5 in the context of the Sigra IST tool (Gray 2000).

The tools used for this include glue in devices such as the Leeman Cell (Leeman, 1968), the CSIRO HI Cell (Worotnicki and Walton, 1976) or the ANZSI cell (Mills and Pender, 1986). All glue in devices have limitations on their use imposed by trying to gain adhesion between the cell and the hole wall in the presence of natural fluids and drilling mud.

The alternative to glue in strain gauge cells are ones that use mechanical contact to measure the diameter change of the pilot hole during the overcore process. The original of these was the USBM deformation cell (Obert, Merrill and Moran, 1962 and Merrill, 1967). The Sigra IST tool has superseded this device for many years (Gray, Wood and Shelukhina, 2013). Both of these tools are 2D devices where the stress acting in the axis of the hole must be estimated.

End of hole devices

These are a category of device that is designed to be glued onto the end of the borehole. They started with the CSIR doorstopper that was used to measure the biaxial stress field perpendicular to the hole. More recently the cone cell has been in use (Obara and Ishiguro, 2004). The latter requires the end of the borehole to be drilled into a cone shape. A glue in cell of matching shape is then glued to the end of the hole. It is then overcored at the diameter of the original hole. Linear elastic theory is used to determine the state of stress in the rock from deformation measurements.

Analysis of pilot hole overcore device results

The drilling of a pilot hole in a stressed rock mass creates stress concentrations. It also introduces fluid pressure into the pilot hole which acts upon its wall. The process of overcoring relieves the rock stress but also introduces fluid pressure to the outside and end of the core. The effects of internal and external fluid pressure components are readily added to the deformations of Equation 11. The complications in analysis come with anisotropy and nonlinearity of elastic behaviour. If the anisotropy is axisymmetric between those properties in the axis of the hole and those perpendicular to it, then analysis is straightforward. This is frequently the case where drilling is conducted perpendicular to a bedding or plane. If the anisotropy is not axisymmetric the problem becomes more difficult. The real complication is where the rock behaves in a nonlinear manner. Detailed analysis of overcoring in nonlinear and generally anisotropic analysis of overcoring requires numerical simulation with multiple iterations with changing material properties and is a complex process.

Equation 11 can be rewritten as Equation 12 for an orthotropic material displaying axisymmetric anisotropy and including the effects of fluid pressure acting on the surfaces of the overcore. Provided the fluid pressure within the pore space of the rock does not change during the overcore process and neither do the poroelastic coefficients, then the effects of poroelasticity do not affect the deformation of the pilot hole. This means that if the assumption is made that hydrostatic fluid pressure is maintained in the borehole during the overcore and the poroelastic coefficients are constant, then poroelastic effects disappear and Equation 12 is valid for porous rock.

$$\delta D_i = \frac{D}{E_2}[(\sigma_2 + \sigma_3) + 2(\sigma_2 - \sigma_3)(1 - v_{23}^2)\cos 2\theta_i - (1 - v_{23})P]$$
$$- \frac{D}{E_1} v_{12}[\sigma_z - P] \tag{12}$$

Where δD_i is the change in pilot hole diameter with overcoring
θ_i is the angle from the axis in which σ_2 acts
P is the fluid pressure in the borehole
v_{23} is the Poisson's ratio across the core (= v_{32} as axisymmetric)
v_{12} is the Poisson's ratio describing negative radial/axial deformation of the core
E_1 is Young's modulus measured in the axis of the overcore
E_2 is Young's modulus measured perpendicular to the core (= E_3 as axisymmetric)

These multiple parameters emphasise the need for careful core testing to determine Young's moduli, Poisson's ratios and poroelastic coefficients. A three to one ratio of stiffness along a bedding plane compared to the axial stiffness makes a large difference to calculated stress. The relationship between Young's moduli and Poisson's ratio for an orthotropic solid given in Equation 13 is useful in determining the values of Poisson's ratio used in Equation 12. Normally v_{23} is not measured in any form of conventional core testing. The paper by Gray, Zhao and Liu, 2018, examines the determination of rock properties in more detail and includes methods to determine v_{23}.

$$\frac{v_{ij}}{E_i} = \frac{v_{ji}}{E_j} \tag{13}$$

In examining Equation 12 it is possible to see that it contains terms to describe the deformation due to the effects of axial stress and fluid pressure. With greater depth these effects become larger.

If the stress at the borehole wall leads to compressive or tensile failure then overcoring cannot be used. There are some exceptions, as a very minor degree of flaking which disrupts the measurement of one pin in the Sigra IST tool can be ignored due to the redundancy of measurement. The small diameter of the pilot hole (26 mm for the Sigra IST tool) means that the stresses within the pilot hole wall can frequently be higher than the uniaxial compressive strength of the sample. The reason for this is simply scale. The core which is typically HQ size (61 mm diameter) is likely to contain more flaws than the pilot hole. This means that borehole breakout in the pilot hole frequently does not occur until stresses are well beyond the uniaxial compressive strength measured using the rock core.

Borehole Breakout

Borehole breakout is caused by compressive failure of the borehole wall brought about by a combination of stress and the stress concentration around a borehole. In terms of linear, elastic isotropic behaviour the zone of breakout is where the tangential stress exceeds the compressive strength of the rock as described in Equation 8. Within this equation there are three unknowns, σ_2, σ_3, and the tangential (compressive) stress at which failure occurred, σ_T. The only known might be the breakout width (θ). These are even difficult to determine in many cases. If we have a homogeneous sandstone then determining the breakout width or depth may be possible. If there is any pre-existing jointing this becomes difficult. It is further complicated by the effects of induced fracturing which is associated with the passage of the bit as part of the drilling process. In crystalline rock the difficulty in measuring breakout width is even greater.

If one is only able to measure one parameter and there are three unknowns then a unique solution cannot be found. The petroleum industry tries to reduce the number of unknowns by using borehole breakout along with hydrofracture which enables the determination of the minimum stress. That reduces the unknowns to two. They then endeavour to link the horizontal strength of the rock to the sonic velocity obtained from borehole geophysical logging. This assumes first that Young's modulus is a function of sonic velocities (compressional and shear). This is theoretically correct, however the relationship between Young's modulus and compressive strength is tenuous. Then with the benefit of examining the width of breakout the practice is to estimate the major stress. This represents a lot of assumptions the basis of which is the stress distribution around a borehole in linearly elastic, isotropic rock.

Figure 6 shows the acoustic scan image of breakout in siltstone. It is relatively even and the width of breakout may be approximately measured. The breakout is however not continuous.

Figure 7 shows an acoustic scan image of breakout in a metasiltstone. The breakout has a much more complex form. It is uneven and clearly influenced by fractures within the rock mass.

THE VARIABILITY OF STRESS IN THE GROUND

The stress in the ground is infrequently uniform. Gray, 2000, presented the concept of tectonic strain. This is the strain within the rock mass required to generate the stress that exists within a rock mass. Tectonic strain explained the different stresses in each layer in terms of stiffness and the tectonic strain to which the strata had been subject. Gray, Wood and Shelukhina, 2013, presented an example of a mine site where the stresses changed direction due to faulting which was followed by subsequent reloading. More work since has shown that the stresses around fault edges are raised in response to the shifting of load from the fault to adjacent areas. Where cooling effects occur the situation becomes more complex.

What can be said with certainty is that the more complex the geology, the more complex the stress distribution is likely to be. The cases where there are uniform stresses are few, there are more likely to be uniform tectonic strains but these change with folding and faulting. Where there are igneous intrusions they may be thought of as giant hydrofractures that indicated the state of minimum stress at the time of intrusion but are highly unlikely to reflect the current stress distribution. When metamorphism occurs the changes in dimension associated with diagenesis are important too.

What is certain is that a few stress measurements are extremely unlikely to present a picture of the real stress distribution.

CONCLUSIONS

This paper has outlined the basis for the four most used stress measurement systems, hydrofracture, hydrojacking, overcoring and borehole breakout. With the exception of the determination of the minimum stress from hydrofracture, all the measurements are based on the stress distribution around a borehole in an elastic, isotropic rock mass. If the rock mass is not isotropic or homogeneous, then there are flaws in all the analyses used. Dealing with the effects of anisotropy, nonlinearity and poroelasticity requires a significant effort. This effort may not always be worth the return and it is probably better to analyse stress measurements based upon the current methods, at least initially, so as to obtain an approximate distribution of stress. Caveats may be placed on the likely accuracy of the measurements. Later those areas that are of concern may be focused on in more detail using more complex analysis if it is warranted.

Stress measurement in rock is difficult and requires interpretation beyond that of each individual test. The author's company is frequently asked to quote to make a single stress measurement at some depth, without reference to the geology. A sensible quotation is difficult to arrive at, and a single measurement is useless to the client because it is quite possible that a few metres away the stress is quite different. There will be a good geological reason for this but without the geology and some distribution of measurement no useful interpretation of measurement may be made. It is not uncommon upon further enquiry to receive core photos of a box of broken core and to be expected to be able to run a precise overcore test in the next borehole.

Figure 8 shows a graph which approximately outlines what test might be undertaken in different rock masses containing yet unknown stresses and fracture spacings. Practically it is best to use every technique that might work in the situation where a stress distribution is required.

ACKNOWLEDGEMENTS

The author wishes to thank those companies that have invested in stress measurements with Sigra over the last 25 years. Much has been learnt during this period. The assistance of Jeff Wood over the years and more recently Xiaoli Zhao has been greatly appreciated.

REFERENCES

Barree, R D, 1998. Applications of pre-frac injection/falloff tests in fissured reservoirs - field examples, paper presented to SPE Rocky Mountain Regional/Low Permeability Reservoirs Symposium, Denver, Colorado. DOI: 10.2118/39932-ms
.
Barree, R D, Barree, V L and Craig, D P, 2009. Holistic Fracture Diagnostics, paper SPE 107877 presented to Rocky Mountain Oil and Gas Technology Symposium, Denver, 16-18 April, (ed: J W Beeston).

Gray, I, 2000. The measurement and interpretation of stress, paper presented to Bowen Basin Symposium 2000: The New Millennium - Geology Proceedings, Rockhampton, 22-24 October.

Gray, I, Wood, J H and Shelukhina, I, 2013. Real stress distributions in sedimentary strata, paper presented to Proceedings of the 6th International Symposium on In-situ Rock Stress, Sendai, Japan, 20-22 August.

Gray, I, Zhao, X and Liu, L, 2018. The determination of anisotropic and nonlinear properties of rock through triaxial and hydrostatic testing, paper presented to Proceedings of the 10th Asian Rock Mechanics Symposium, Singapore, 29 October to 3 November.

Hagoort, J, 1981. Waterflood-induced hydraulic fracturing, PhD Thesis, Delft University, Delft, Netherlands.
Jaeger, J C and Cook, N G W, 1979. Fundamentals of Rock Mechanics, 3rd edition (Chapman and Hall: London).

Kirsch, E G, 1898. Die Theorie der Elastizität und die Bedürfnisse der Festigkeitslehre. Zeitschrift des Vereines deutscher Ingenieure, 42, (797–807)

Leeman, E R, 1968. The determination of the complete state of stress in rock using a single borehole-laboratory and underground measurement, International Journal of Rock Mechanics and Mining Sciences, 5:pp 31-56.

Leeman, E R, 1971. The CSIR "doorstopper" and triaxial rock stress measuring instruments, Rock Mechanics, 3:pp 25-50.

Merrill, R H, 1967. Three-component borehole deformation gage for determining the stress in rock, U.S. Dept. of the Interior, Bureau of Mines, Washington, D.C.

Mills, K W and Pender, M J, 1986. A Soft Inclusion Instrument For In Situ Stress Measurement In Coal, paper presented to International Symposium on rock stress and rock stress measurements, Stockholm, Sweden, 31 August 1986.

Nolte, K G, 1979. Determination of fracture parameters from fracturing pressure decline, Paper SPE 3814, paper presented to Annual Technical Conference and Exhibition, Las Vegas, NV, 23-26 September.

Obara, Y and Ishiguro, Y, 2004. Measurements of induced stress and strength in the near-field around a tunnel and associated estimation of the Mohr-Coulomb parameters for rock mass strength, International Journal of Rock Mechanics and Mining Sciences, 41(5):pp 761-769.

Obert, L, Merrill, R H and Moran, T A, 1962. Borehole Deformation Gauge for Determining the State of Stress in Rock, US Bureau of Mines Investigation, RI 5978.

Worontnicki, G and Walton, R J, 1976. Triaxial hollow inclusion gauges for determination of rock stresses in situ, paper presented to Symposium on Investigation of Stress in Rock : Advances in Stress Measurement, Sydney, Australia, (ed: A. J. Hargraves), pp 1-8.

FIGURES

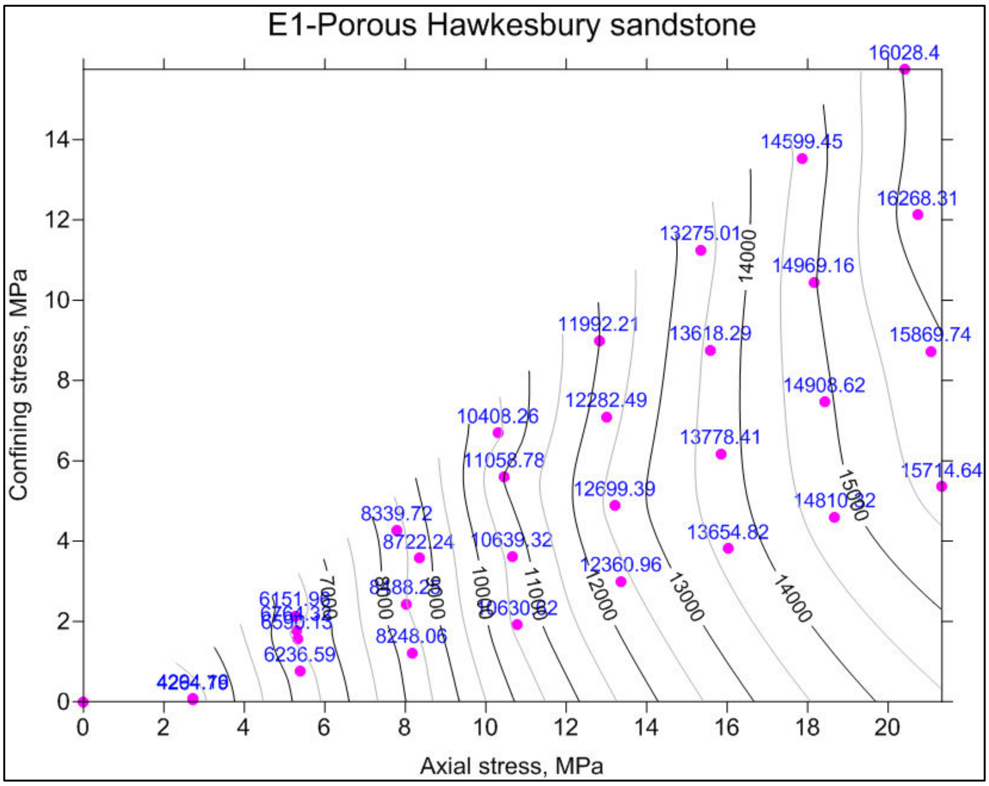

Figure 1. Axial Young's modulus from a porous sandstone.

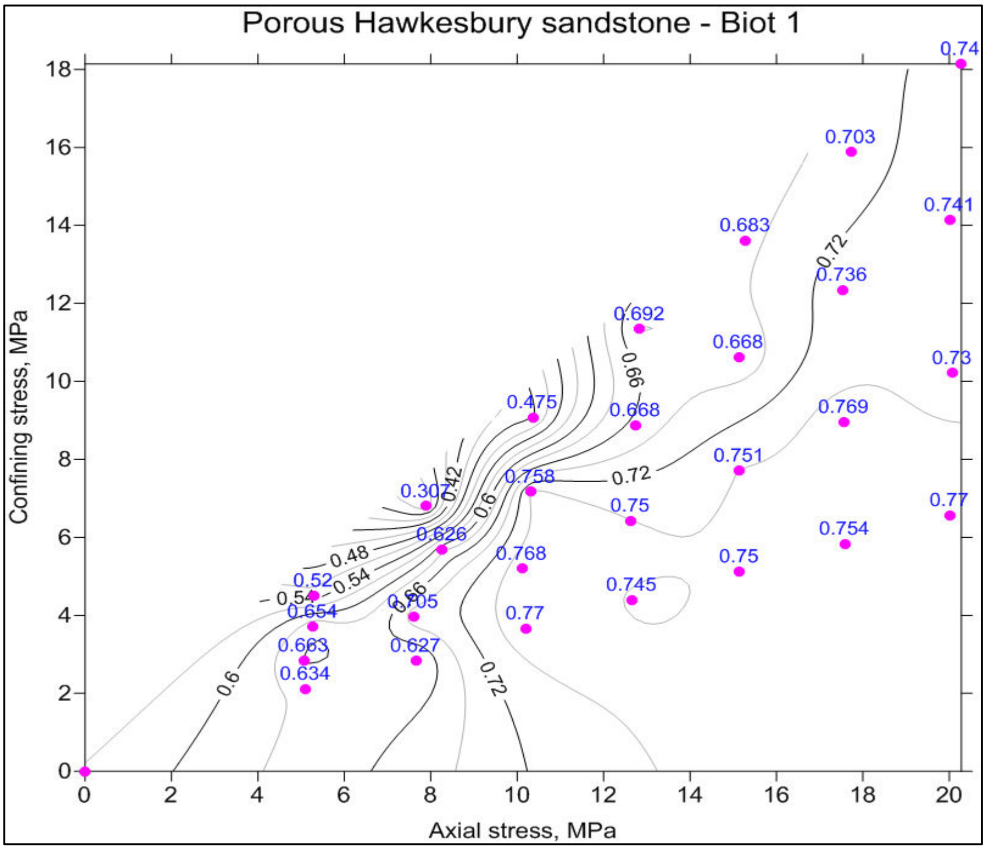

Figure 2. Poroelastic coefficient in axial direction from a porous sandstone.

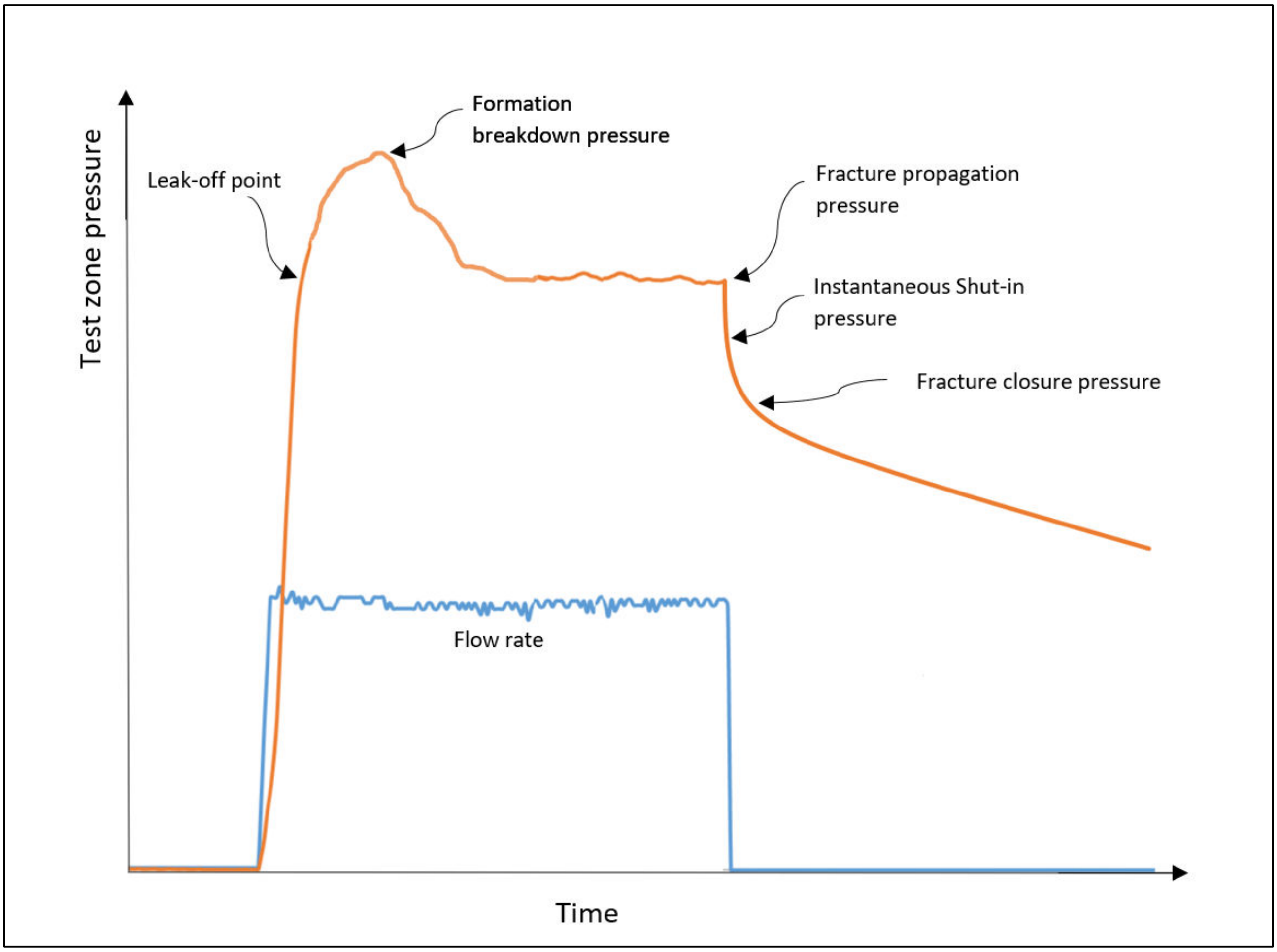

Figure 3. Example of hydrofracture pressure response.

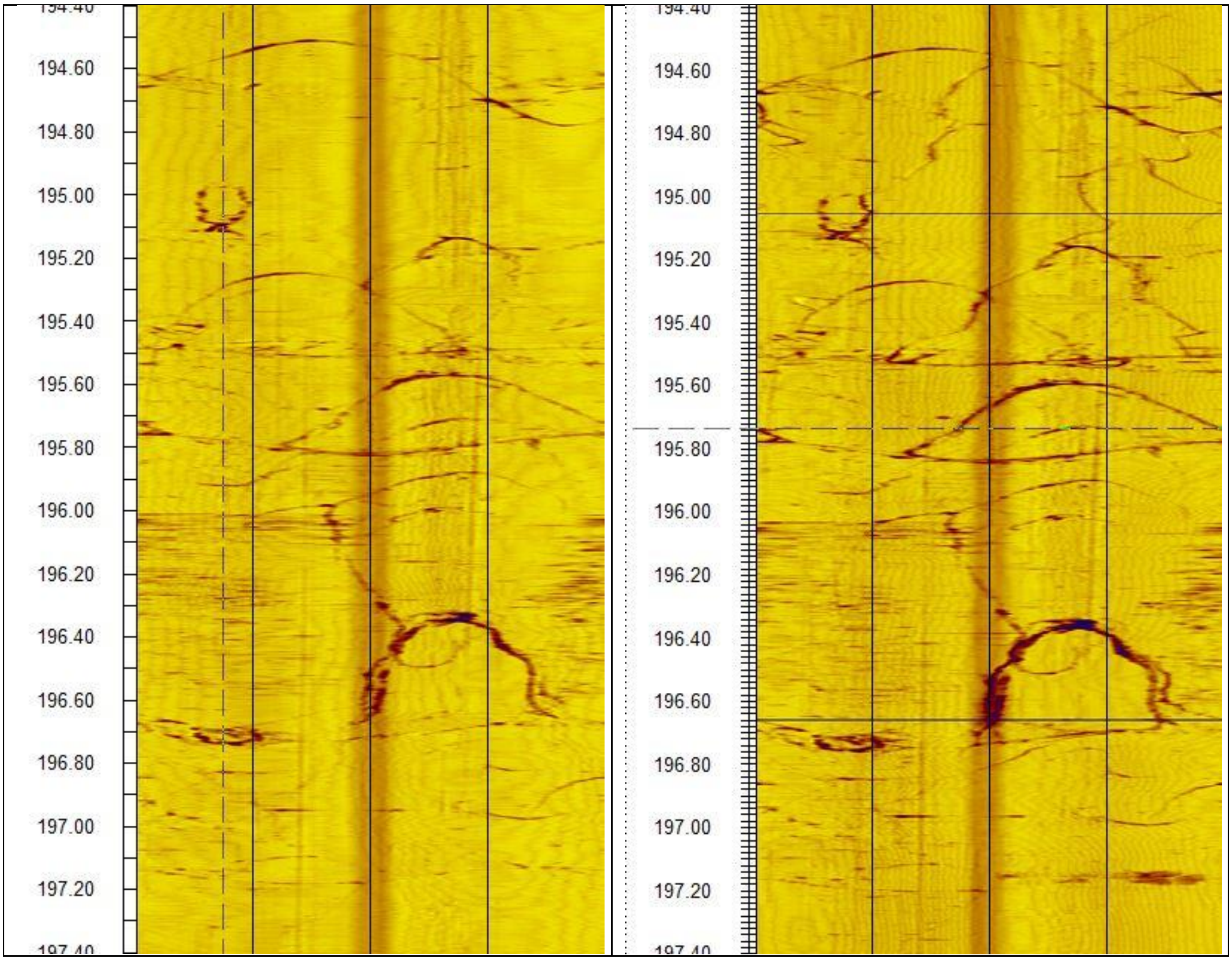

Figure 4. Acoustic scans of a borehole wall containing multiple fracture sets before (left) and after (right) hydrojacking.

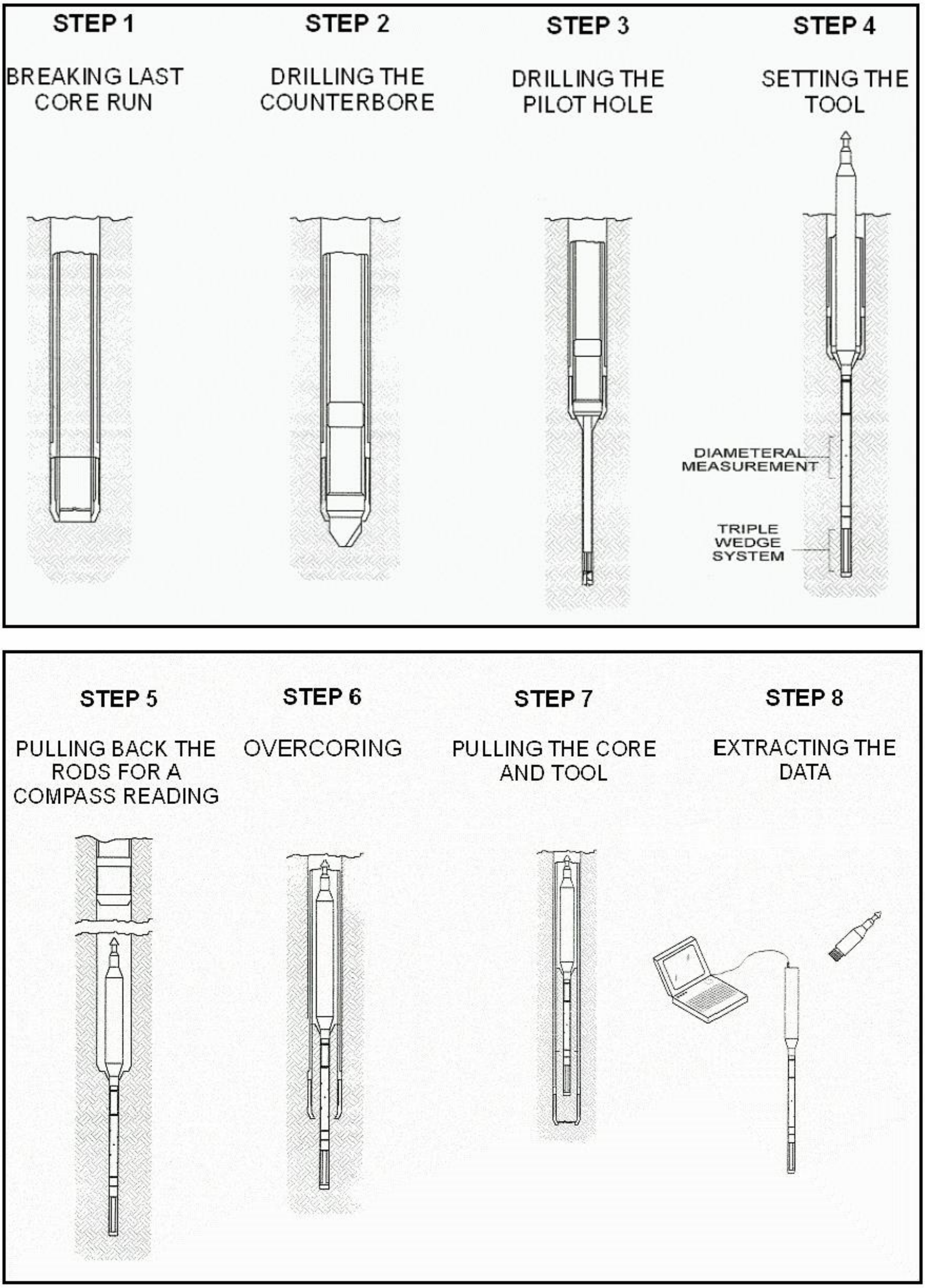

Figure 5. The overcore process using the Sigra IST tool

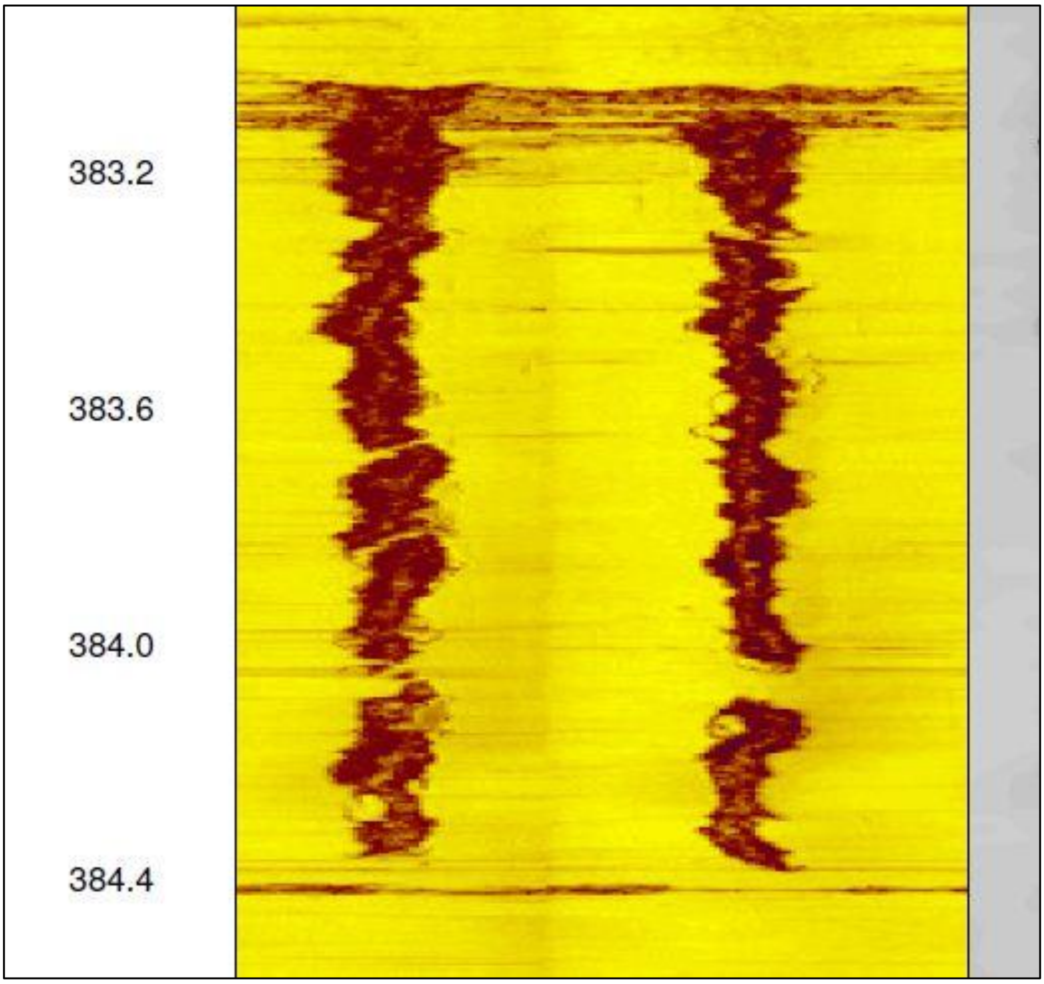

Figure 6. Acoustic scan image of borehole breakout in siltstone. Image from 0 to 360° in borehole.

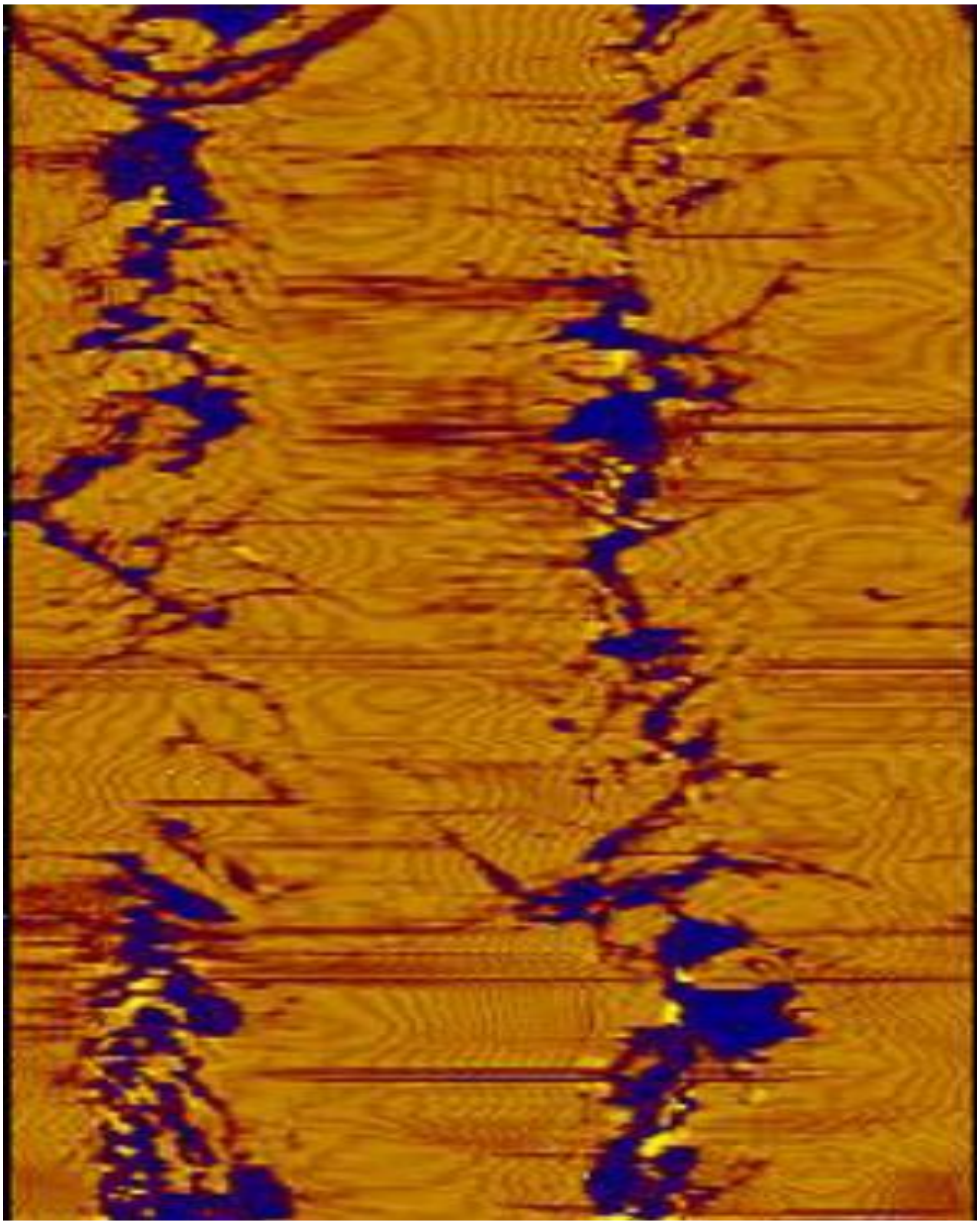

Figure 7. Acoustic scan image of breakout in metasiltstone. Image from 0 to 360° in borehole.

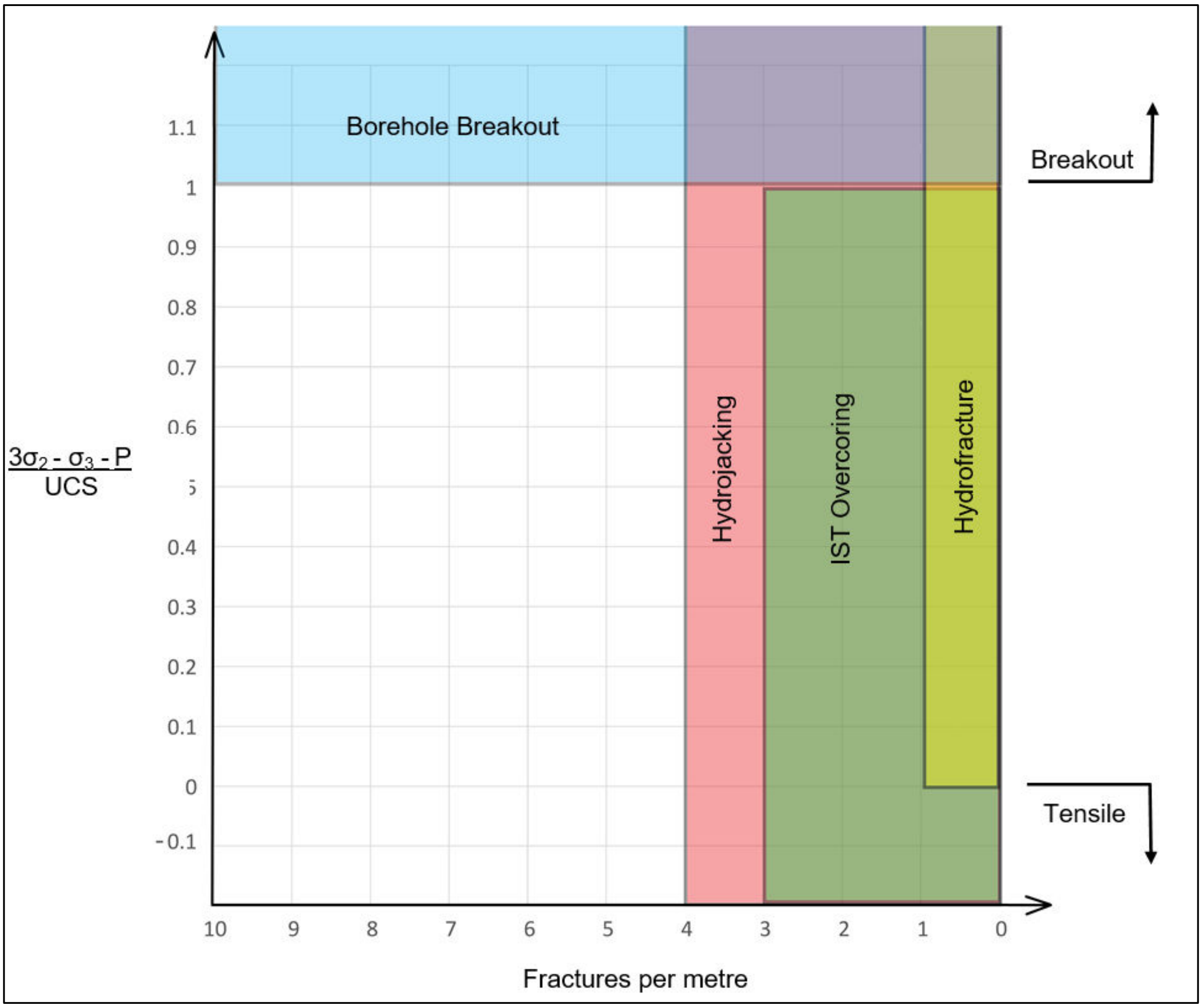

Figure 8. An indication of what technique for stress measurement might be used in terms of stress and fractures.